 ISSN 2579-7298

Expert System for Diagnosis of Lung Disease from X-Ray Using CNN and SVM

Zulkifli Zulkifli[a,1], Retno Ariza S[b,2], Sfenrianto[c,3], Zulvi Wiyanti[d,4], Panji Bintoro[e,5,*], Fitriana Fitriana[f,6], Sukarni Sukarni[g,7], Nopi Anggista Putri[h,8] , Dwi Yana Ayu Andini[i,9]

[a] Informatics Engineering, Faculty of Technology and Informatics, Aisyah University, Indonesia
[b] Faculty of Medical, Lampung University, Indonesia
[c] Information Systems Management, Binus University, Indonesia
[d] Midwifery, Prima Nusantara Bukittinggi University, Indonesia
[e,i] Software Engineering, Faculty of Technology and Informatics, Aisyah University, Indonesia
[f,g,h] Midwifery, Faculty of Biomedical Science, Aisyah University, Indonesia
[1] zulkifli@aisyahuniversity.ac.id; [2] arizapulmo@gmail.com; [3] sfenrianto@binus.edu; [4] zulviwy@gmail.com; [5] panjibintoro09@aisyahuniversity.ac.id *;
[6] fitriana@aisyahuniversity.ac.id; [7] sukarni@aisyahuniversity.ac.id; [8] nopianggista@aisyahuniversity.ac.id; [9] dwiyana@aisyahuniversity.ac.id
* corresponding author

ARTICLE INFO

Article history
Received 29 Jul 2023
Revised 08 Sep 2023
Accepted 12 Des 2023

Keywords
Expert System
Lung Disease Diagnosis
Convolutional Neural Network
Support Vector Machine

ABSTRACT

The lung disease diagnosis expert system utilizes human knowledge to diagnose various conditions affecting the lung. Diseases caused by fungal or bacterial infection in the organ can cause inflammation as well as death when it is not detected on time. A standard method to diagnose these conditions is the use of a chest X-ray (CXR), which requires careful examination of the image by an expert. In this study, several CNN and SVM architectural models were proposed to classify CXR images to diagnose whether a person has COVID-19, Viral Pneumonia, Bacterial Pneumonia, Tuberculosis (TB), and Normal. The experiment showed that InceptionV3 had the best results compared to other CNN architectures and SVM. Classification accuracy, precision, recall, and f1-score of CXR images for COVID-19, Viral Pneumonia, Bacterial Pneumonia, TB, and Normal were 0.86, 0.91, 0.91, and 0.91, respectively. This study was based on a deep learning system with different CNN and SVM architectures that can work well on the CXR images dataset for diagnosing lung disease.

1. Introduction

Expert systems, a major center of artificial intelligence (AI), are currently used in many fields to solve problems by drawing on human knowledge [1][2]. It is also employed in different fields, including medicine to diagnose diseases. Smoking, air pollution, or bacterial infections, which can harm the respiratory system and result in major issues, are the usual causes of diseases of the human organs, notably the lungs. Previous reports showed that a total of 212.3 million people had lung disease in 2019 globally, with 74.4 million death cases[3]. These conditions can cause a natural weakness in the respiratory system, which requires carefulness and attentiveness from the patients to alleviate the problem [4]. Chest X-ray (CXR) images have the potential to monitor and examine lung diseases, such as Pneumonia, Tuberculosis (TB), and COVID-19[5].

2019's Coronavirus Disease (COVID-19) is an infectious illness brought on by a rare virus[6], which follows various past epidemics by highly contagious respiratory viral infections[7]. The first reported case occurred in Wuhan, China, in December 2019 and it has gained global attention, specifically in the health sector [8][9]. Pneumonia is an infectious disease caused by viruses, microbes, fungi, and bacteria. Furthermore, it can also compromise the lungs, and this is dangerous

and life-threatening when not identified early[10][11]. Pneumonia has caused more than 1.1 million hospitalizations as well as 50,000 deaths in 2010 of which the majority occurred in patients over 65 years old. Tuberculosis is an infectious bacterial disease that can spread through direct contact or air[12][13]. It often attacks the lungs, but can also infect other organs, such as the kidneys, bones, spine, and brain. 4,3 million people were estimated to have TB infection in 2020, and 700.000 cases of TB-related deaths are predicted[9].

CXR is the most common clinical method for diagnosing lung disease, but can be very challenging, even for radiologists. The patients' X-ray results for COVID-19, Pneumonia, and TB are often unclear, and this inconsistency causes several subjective decisions among radiologists[14]. Therefore, it is necessary to have a support system to help radiologists diagnose these conditions from CXR images[15]. In the field of deep learning image processing, Convolutional Neural Network (CNN), a key technology, has received great attention. After AlexNet's great success, performance improvement models, such as VGG, ResNet, and InceptionNet are constantly evolving, and new studies are still been carried out to occupy the State-of-the-Art[16].

In another study, various deep learning-based approaches use CXR images to support the diagnosis of lung disease[17], and CNN was proposed for the classification of the results. The study developed a small-sized CNN architecture because the previously trained model was difficult to apply. A total of 12 classes of CXR datasets were used, with an 86% accuracy score in the test[18], also proposed a deep learning-based approach. The VGG-19 model can be applied to develop suitable deep learning-based COVID-19 detection methods with the limited illness dataset. The categorization of COVID-19 vs. Pneumonia and Pneumonia vs. Normal conditions for a number of imaging modalities, including X-ray, ultrasound, and CT scan, is also made easier with the use of the model.

A detailed study has been carried out[19][20], to show the importance of lung disease treatment, specifically COVID-19 and Pneumonia. Apart from its problem-solving abilities, CNN also provides breast cancer detection[21][22], brain tumour segmentation[23][24], diagnosis of Alzheimer's disease, and skin lesions classification[25][26]. Deep learning has been used in several studies for the detection of lung disease. [27]proposed a CNN of different architecture to extract features from CXR images and classify them to detect whether a person has pneumonia. The experiments were performed to assess the architectural performance and the augmented data effect showed that CNN with trained dropouts perform better than other models. [12]applied two techniques, namely CNN and ANN to diagnose TB, and they produced promising results. The ANN network with ResNet50, GLCM, DWT, and LBP features achieved 99.22% accuracy, 99.23% sensitivity, and 99.41% specificity. [28]added more synthesis data argumentation variability to the dataset by enlarging it. CovidGAN was utilized to create artificial CXR pictures, and ACGAN and CNN were developed to increase classification performance, resulting in 95% accuracy. Furthermore, [6]proposed an end-to-end system to identify COVID-19 and localize the diseased areas from two pictures obtained using several medical modalities. The study enhanced the Inception Recurrent Residual Neural Network (IRRCNN) in the utilized NABLA-3 network model for classification and segmentation. Then, using openly accessible data sets, it was evaluated on X-ray, abdominal CT, and full-body CT images. The observed results demonstrated encouraging detection results with test accuracy for COVID-19 from X-ray and CT images of 84.67% and 98.87%, respectively. [29] investigated the use of deep learning transfer to classify Pneumonia on CXR images. The experimental results showed that fine-tuning the learning transfer increases the performance from the initial training. The proposed models, ResNet50, InceptionV3, and DenseNet121, are trained separately through the learning transfer from scratch. The test results reached 4.1% to 52.5% of the area under the curve (AUC), which was larger compared to previous studies.

This is a comparative study of deep learning using CNN involving several architectures and machine learning with SVM and feature extraction using PCA, which was implemented into an application with an expert system. The presentation was organized as follows: Section 2 shows the research flow and the methods used, while 3 reveals the results and discussions. Furthermore, section 4 presents the conclusions.

2. Research Method

2.1. Proposed Method

The proposed method is illustrated in Figure 1, where CXR images were used as input for diagnosing Pneumonia and COVID-19.

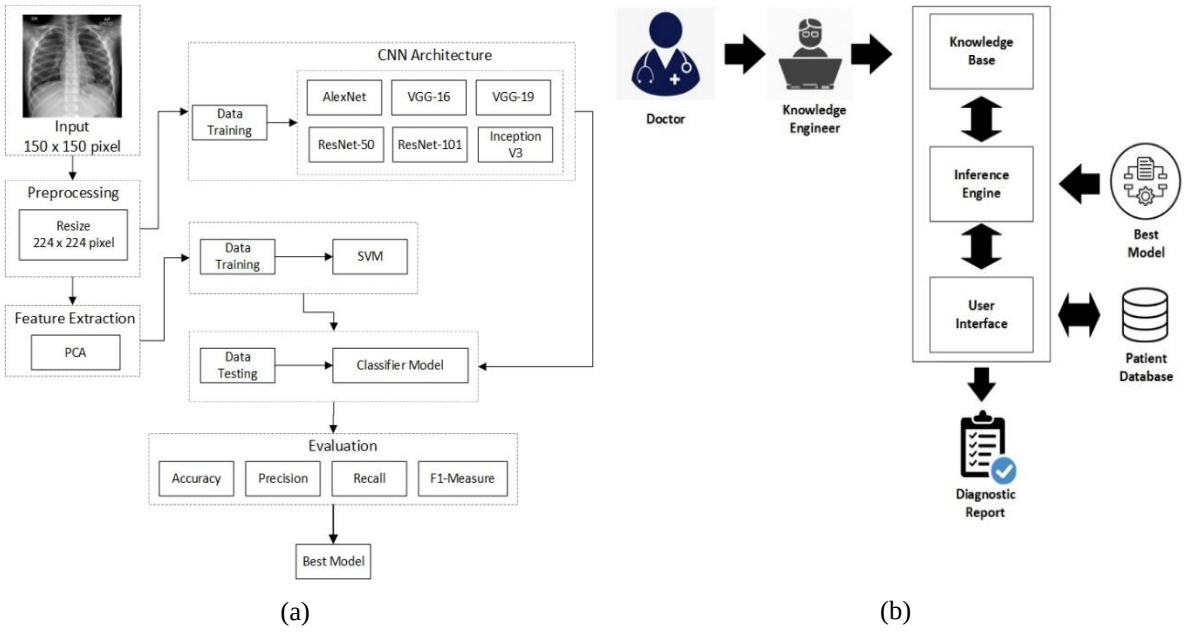

(a) (b)

Fig. 1. (a) Illustration of proposed methodology for diagnosis of lung disease, (b) Illustration of lung disease diagnosis system.

Figure 1a shows the initially entered CXR images were initially resized to 224 x 224 pixels for compatibility with CNN and SVM models. In deep learning, the CNN architectures used for diagnosing Pneumonia and COVID-19 include AlexNet, VGG16, VGG19, ResNet50, ResNet101, and InceptionV3. Meanwhile, in machine learning, PCA extraction feature with SVM as the classifier were implemented. To obtain the best model, CNN and SVM performance was evaluated using accuracy, precision, recall, and f1-measure. Figure 1b shows an illustration of a lung disease diagnosis system.

Medical knowledge from specialist doctors was required to develop an expert system. This knowledge was collected in two phases, where lung disease medical background was obtained through personal interviews with specialist doctors and patients in the first stage. A set of rules was then created in which each of them contains diseases that occur in the lungs. The data obtained were then collected and stored in the knowledge base, which were also connected to an inference engine that processes rules to infer facts. Programmers or engineers generally use inference engines to construct the best model for predicting lung disease. They are then linked to the user interface to gather patient data. Programmers or knowledge engineers who store the data in a database also created the user interface. Patients' data and diagnostic results became the system's final output.

2.2. Dataset Descriptiom

This experiment was carried out using CXR images dataset with Bacterial Pneumonia, Viral Pneumonia, COVID-19, Tuberculosis, and Normal diseases obtained from the online data repository.

2.3. Convolutional Neural Networks (CNNs)

The primary components of the CNN architecture were built using a series of convolution, normalization, and pooling layers [30][31]. The convolution layer was in charge of feature

extraction and normalization in the interim[32]. The pooling part was used for local features normalization and the down-sampling of the respective local features[5][19].

The convolution layer operates by slicing the image into discrete fields, or receptive fields, as they are often called. The extraction of motifs is aided by the image's split into small blocks, and Equation (1) displays the feature map produced [33].

$$F_l^k = [f_l^k(1,1), \ldots, f_l^k(p,q), \ldots, f_l^k(P,Q)] \quad (1)$$

Where F_l^k is the input feature matrix for l^{th} layer and k^{th} kernel. The pooling layer was used for the down-sampling of the feature map. Various techniques were also applied for the process, namely the average and maximum [5]. The operation process is defined, as shown in Equation (2).

$$Z_l^k = g_p(F_l^k) \quad (2)$$

Where Z_l^k is the input feature matrix for l^{th} layer and k^{th} kernel, the fully connected layer (FC) has a full connection to all activation in the previous layer. Additionally, the FC offers discriminatory characteristics for categorizing the input image into different groups. The optimization method used in CNN training is similar to that used in classical machine learning. Two well-known techniques for neural network training include Adaptive Moment Estimation (ADAM) and Stochastic Gradient Descent with Momentum (SGDM).

AlexNet or the Traditional [34] has a five-layer convolution with three pooling, two fully connected, and a softmax layer. Furthermore, VGG16 and VGG19 [18][35] are CNN architectures with very small convolutional filters of 3 x 3, and stride 1 was designed to achieve high accuracy in big-scale image recognition. In the implementation, VGG16 and VGG19 have differences in the convolution depth or max pooling and fully connected layers, namely 16 and 19, respectively.

In ResNet50 and ResNet101 [18][36] The CNN algorithm was created as a way to design a system that traverses across the layers without losing the gradients that are inherent in deep neural networks. As a result of this architecture, the network becomes more effective at learning, enabling the building of deeper networks and improving model accuracy. Networks having 50 and 101 layers, respectively, are called ResNet50 and ResNet101.

InceptionV3 [18][37] By widening and deepening the network, CNN hopes to boost the network's computing capacity. Furthermore, jump connections were employed as the building blocks of efficient structures that network designers referred to as "inception modules."

Define abbreviations and acronyms the first time they are used in the text, even after they have been defined in the abstract. Abbreviations such as IEEE, SI, MKS, CGS, sc, dc, and rms do not have to be defined. Do not use abbreviations in the title or heads unless they are unavoidable.

2.4. Principal Component Analysis (PCA)

Application areas for PCA include data visualization, feature extraction, data compression, and dimensionality reduction. Additionally, it enables the conversion of a set of X-correlated variables into a smaller number y, specifically the uncorrelated variable known as the component principal with y < X, while preserving the same level of variability as the original data. One of the PCA features is an image compression technique that reduces the size while maintaining the maximum possible quality[38][39]. The steps involved in PCA are:

With the exception of labels, all dataset dimensions are calculated by standardization[28]. Because the data are scaled, each variable makes an equal contribution to the study. In Equation (3) below, z is the scale value, x is the initial, and is the mean and standard deviation.

$$z = \frac{x - \mu}{\sigma} \quad (3)$$

Covariance Matrix Computation: Covariance was measured between 2 dimensions[28]. In a 3-dimensional data set (A, B, C), its level between dimensions A and B, B and C, as well as A and C are measured. Equation (4) was used to compute the covariance between X and Y.

$$Cov(X,Y) = \frac{1}{n-1}\sum_{i=1}^{n}(X_i - X')(Y_i - X') \quad (4)$$

Calculate Eigenvectors and Corresponding Eigenvalues: For the covariance matrix, eigenvectors and corresponding eigenvalues were computed[28]. Furthermore, the eigenvectors are scaled according to the appropriateness of the eigenvalues. The vector u, which fulfills the following equation (5), is the eigenvector of the matrix A.

$$Au = \lambda u \tag{5}$$

Where λ is the eigenvalue. This means that the linear transformation formation is defined and can be rewritten in Equation (6), as follows:

$$(A - \lambda I)u = 0 \tag{6}$$

Where I is the identity matrix.

2.5. Support Vector Machine (SVM)

Based on statistical learning theory, SVM is a two-class classification technique. For n-dimensional space, the input data $x_i\ (i = 1 \dots k)$ belongs to classes 1 or 2. The label -1 corresponded to class 2, while -1 and +1 were for classes 1 and 2, respectively[40]. When the input data can be separated linearly, the hyperplane separation can be shown in Equation (7).

$$f(X) = w^T x + b \tag{7}$$

Where b is the scalar or bias value and w is the n-dimensional weight vector. The largest margin between the positive and negative classes is determined by this equation. Equation (8) displays the choice function.

$$f(x) = sgn(w^T x + b) \tag{8}$$

Equation (9) identifies the hyperplane that meets the largest margin between the two classes when the two classes can be separated linearly.

$$\begin{Bmatrix} Minimize & \frac{1}{2}||w||^2 \\ Subject\ \ to & y_i\ (w_i\ x_i + b)\ \geq 0 \end{Bmatrix} \tag{9}$$

When the SVM parameters are set properly, the performance classification improves. SVM training was performed by resolving Equation's (10) optimization issue.

$$\begin{Bmatrix} MaximizeL(\alpha) = \sum_{i=1}^{k} \alpha_i - \frac{1}{2}\sum_{i,j=0}^{k} \alpha_i \alpha_j y_i y_j K(x_i, x_j) \\ Subject\ \ to\ \ \sum_{i=1}^{k} y_i\ \alpha_i = 0\ \ \alpha_i \geq 0\ for\ i = 1 \dots k \end{Bmatrix} \tag{10}$$

Where $K(x_i, x_j)$ is the kernel function, $\propto_i$ is the Lagrange multiplier. When the data cannot be separated linearly, the kernel function mapping changes according to Equation (11).

$$K\ (x_i, x_j) = K\ (x_i, x_j) + \frac{1}{C}\delta_{ij} \tag{11}$$

Where C is the penalty parameter and its appropriate value can improve the classification performance, while $\delta_{ij}$is the Kronecker symbol. In this study, the kernel function is radial based, and this function is given in Equation (12).

$$K\ (x_i, x_j) = exp(-\left|\left|x_i - x_j\right|\right|^2 / (2\sigma^2)) \tag{12}$$

Where σ is the kernel parameter, which affects the data complexity distribution in the feature space.

2.6. Evaluation Metrics

The performance matrices used in evaluating the proposed method include Accuracy, Precision, Recall, and F1-Score[41][42]. Subsequently, it was compared with several proposed models, such as AlexNet, VGG16, VGG19, ResNet50, ResNet101, InceptionV3, and PCA using SVM.

$$\frac{TP + TN}{TP + FP + FN + TN} \quad (13)$$

$$\frac{TP}{TP + FP} \quad (14)$$

$$\frac{TP}{TP + FN} \quad (15)$$

$$2 * \frac{(Recall * Precision)}{(Recall + Precision)} \quad (16)$$

Equation (13) was used to measure the accuracy of the model, while Equation (14) determined the performance in model precision. Furthermore, Equation (15) assessed sensitivity or called recall, and Equation (16) was used to determine the f1-Score.

3. Results and Discussion

On Google Colab, the Python programming language was used for all coding. Additionally, image data were gathered from the source, and a professional applied the CXR label. A total of 80 COVID-19, 664 Viral Pneumonia, 763 Bacterial Pneumonia, 120 TB, and 743 normal (healthy) CXR images were used. In the experiments, 90% of the randomly selected dataset were used for training purposes, and the remaining 10% tested the proposed method. Figure 2 shows some samples of COVID-19, Viral Pneumonia, Bacterial Pneumonia, TB, and normal (healthy) CXR images.

(a) (b) (c) (d) (e)

Fig. 2. Various chest x-ray images (a)COVID-19, (b)Viral pneumonia, (c)Bacterial pneumonia, (d)Tuberculosis, (e)Normal

3.1. Model Training Methodology

In the CNN model, every layer plane increment was trained using Adam's optimization with typical performance parameters. (β1=0.9, β2=0.999, decay=0.0) using a batch size of 32 and running the 50 epochs through the entire dataset. The addition of an effective learning rate scheduling called "ReduceLROnPlateau" defines the search for relevance control of reliability loss. It starts with a learning rate of 0.0001 on demand.

PCA feature extraction reduces image dimensions (n_components=153), which produces in a 0.911 variation ratio. The result of n_components was used as training data for SVM. In the SVM model, several parameters are used, such as kernel='rbf', C=1, class_weight='balanced', and gamma='scale'. The pick was made based on GridSearch's best estimation.

3.2. Result of Model CNN and SVM

The study experiment used six CNN models, namely AlexNet, VGG16, VGG19, ResNet50, ResNet101, InceptionV3, and SVM. Figures 3 and Table 1 show the results of the six models that have been trained and tested.

Table 1. Training and Testing Accuracy of Different Model Architecture CNN

Model	Architecture	Training Accuracy	Testing Accuracy
CNN	AlexNet	0.73	0.71
	VGG16	0.81	0.76
	VGG19	0.81	0.79
	ResNet50	0.83	0.80
	ResNet101	0.86	0.84
	InceptionV3	0.84	0.85

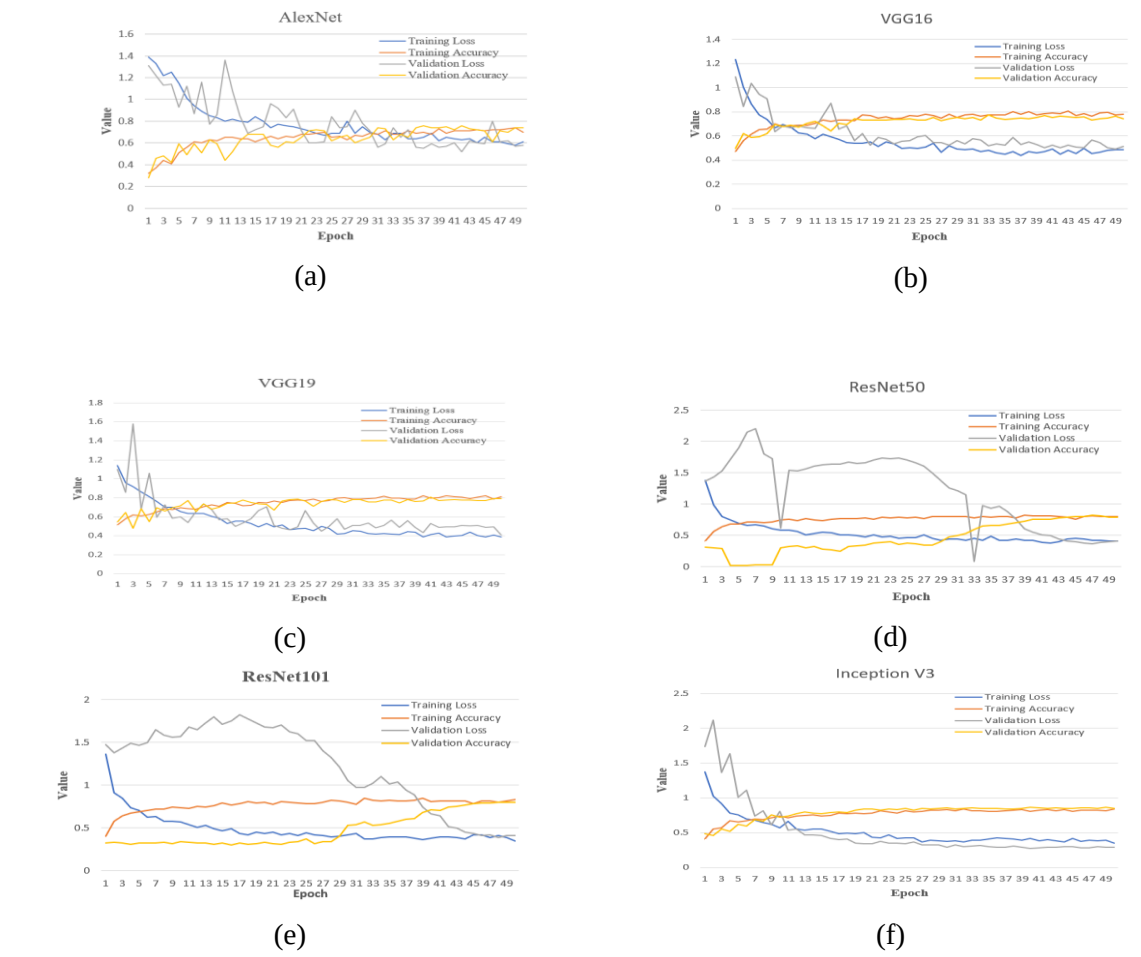

Fig. 3. (a) Performance of AlexNet CNN, (b) Performance of VGG16 CNN, (c) Performance of VGG19 CNN, (d) Performance of ResNet50 CNN, (e) Performance of ResNet101 CNN, (f) Performance of InceptionV3 CNN

Table 1 shows that the CNN ResNet101 model had the highest accuracy scores of 0.86 and 0.84 for training and testing, respectively, while the lowest of 0.73 and 0.71 were obtained from the Traditional variant. The learning curves for each CNN architectural model are shown in Figures 4 to 9. The training curves for the experimental VGG16 and VGG19 are close to the ideal, while that of ResNet50 and ResNet101 was very good. The ResNet101 almost matches the learning results obtained by the InceptionV3. The training curve for the traditional architectural model experiment shows some signs of erratic learning patterns. This was the anticipated outcome, considering the significant variation in the X-ray images dataset. The next experiment was a combination of PCA with SVM classification, as shown in Table 2.

Table 2. General Performance of The SVM Classifier

Model	Parameter	Accuracy
PCA-SVM	(rbf; C=1; balanced; scale)	0.60
PCA-SVM	(rbf; C=100; balanced; scale)	0.58
PCA-SVM	(poly; C=5; balanced; scale)	0.59
PCA-SVM	(poly; C=100; balanced; scale)	0.58
PCA-SVM	(linear; C=5; balanced; scale)	0.54

By computing the difference between the kernel and SVM parameters, the outcomes for the PCA-SVM approach were compiled and displayed in Table 2. The best results were obtained from the the rbf kernel, C=1; class_weight= balanced; and gamma=scale with an accuracy score of 0.60. Therefore, the confusion matrix and classification report can be presented.

3.3. Result of Evaluation Metrics

The proposed model was evaluated using a confusion matrix, such as accuracy, precision, recall, and f1-score. The CNN architectural model was evaluated using CXR with 409 images. The test image contains 131, 21, 121, 10, and 126 cases of Bacterial Pneumonia, COVID-19, normal, Tuberculosis, and Viral Pneumonia, respectively. Table 3 shows each architectural model comparison, while their confusion matrix are presented in Figures 4.

Table 3. The Performance Comparison Evaluation Result of The CNN Architecture Model

Architecture	Accuracy	Precision	Recall	F1-score
AlexNet	0.65	0.78	0.77	0.75
VGG16	0.76	0.84	0.83	0.83
VGG19	0.79	0.86	0.86	0.86
ResNet50	0.80	0.87	0.87	0.87
ResNet101	0.81	0.88	0.88	0.88
InceptionV3	0.86	0.91	0.91	0.91

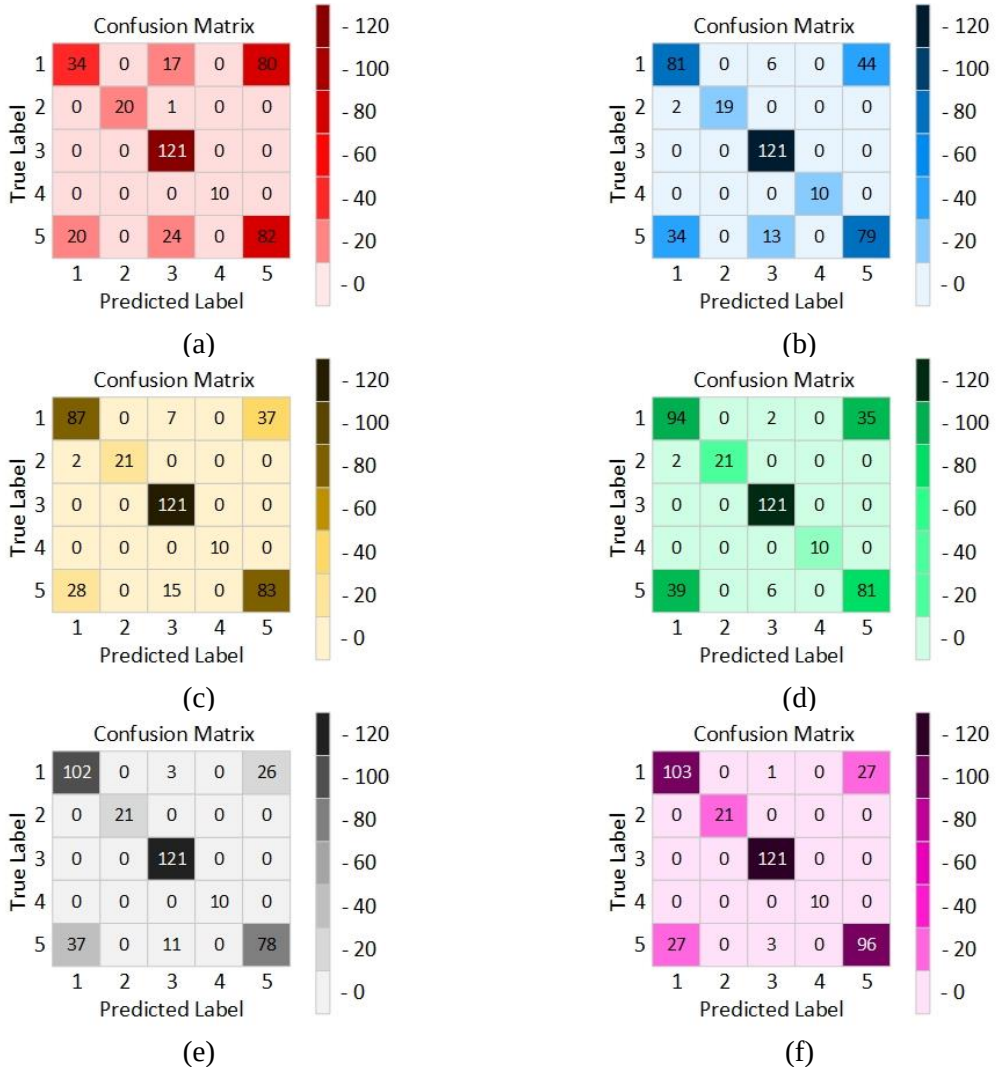

Fig. 4. Confusion matrix (a) Confusion Matrix of AlexNet CNN, (b) Confusion Matrix of VGG16 CNN, (c) Confusion Matrix of VGG19 CNN, (d) Confusion Matrix of ResNet50 CNN, (e) Confusion Matrix of ResNet101 CNN, (f) Confusion Matrix of InceptionV3 CNN

Table 3 shows that all CNN architectural models have classification accuracy scores. InceptionV3 generated the highest score of 0.86, while ResNet101 came in second with a score of 0.81. Furthermore, accuracy scores of 0.80, 0.79, 0.76, and 0.65 were obtained from ResNet50, VGG19, VGG16, and Traditional CNN models, respectively. Figures 4 show the confusion matrix

of all CNN architectural models. In the confusion matrix, classes 0, 1, 2, 3, and 4 were cases of Bacterial Pneumonia, COVID-19, normal, TB, and Viral Pneumonia, respectively. The most optimal results obtained by the InceptionV3 architectural model and its confusion matrix are shown in Figure 4(f). The number of cases of Bacterial Pneumonia, COVID-19, Normal, TB, and Viral Pneumonia that were successfully classified 103 out of 131, 21 out of 21, 121 out of 121, 10 out of 10, and 96 out of 126, respectively. The next evaluation was a combination of PCA with SVM classification. The PCA-SVM combination model using CXR with a total of 558 images was evaluated. Furthermore, the test image contains 178, 51, 144, 38, 147 cases of Bacterial Pneumonia, COVID-19, normal condition, TB, and Viral Pneumonia, respectively. Table 4 shows the evaluation results of the combination of PCA with SVM classification, while the confusion matrix for each PCA-SVM model with different parameter variations are presented in Figures 5.

Table 4. The PCA and SVM Combination Evaluation Results

Parameter	Accuracy	Precision	Recall	F1-score
(rbf; C=1; balanced; scale)	0.60	0.56	0.52	0.53
(rbf; C=100; balanced; scale)	0.58	0.51	0.47	0.48
(poly; C=5; balanced; scale)	0.58	0.51	0.47	0.48
(poly; C=100; balanced; scale)	0.59	0.49	0.47	0.47
(linear; C=5; balanced; scale)	0.54	0.45	0.44	0.44

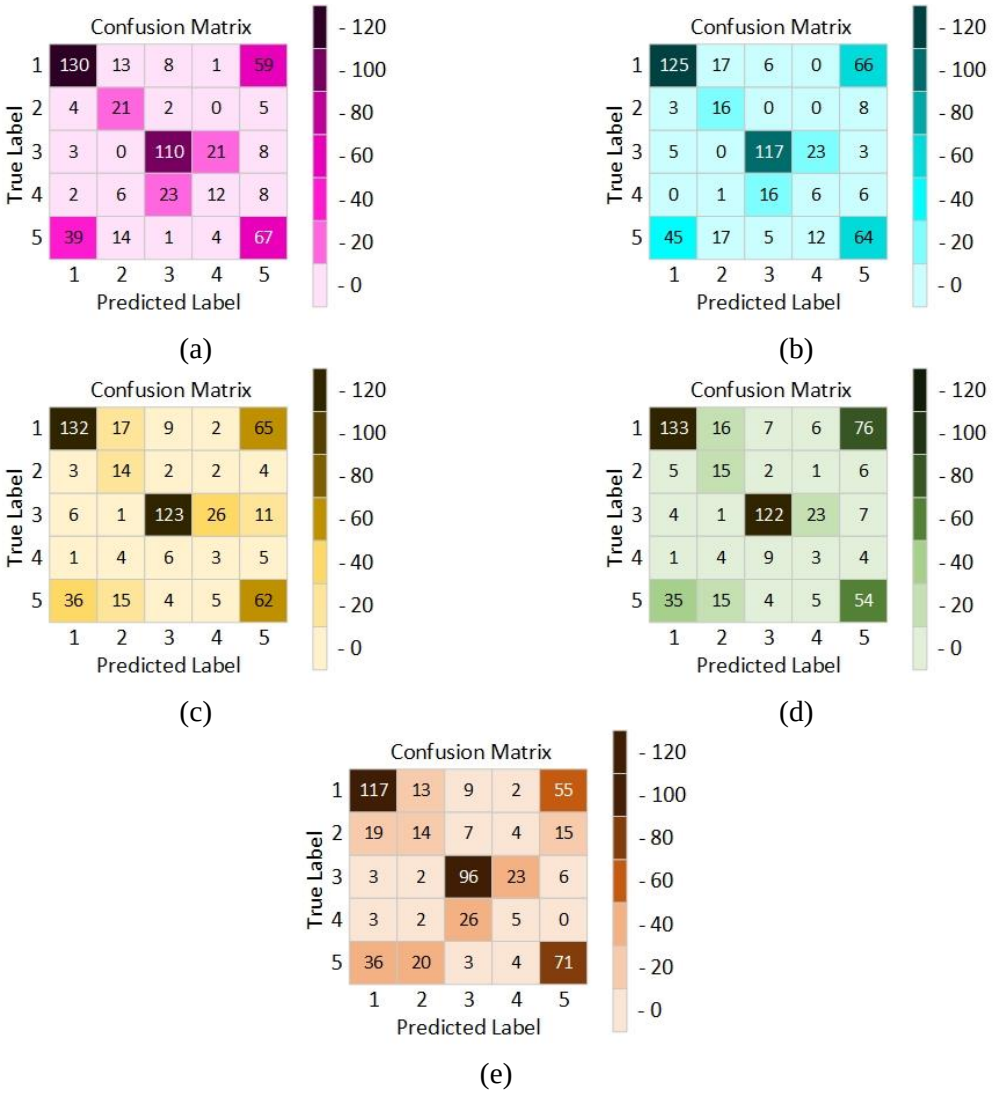

Fig. 5. Confusion matrix of PCA-SVM (a) (rbf; C=1; balanced; scale), (b) (rbf; C=100; balanced; scale), (c) (poly; C=5; balanced; scale), (d) (poly; C=100; balanced; scale), (e) (linear; C=5; balanced; scale)

Table 4 shows that all PCA-SVM combinations have obtained classification accuracy scores. The highest of 0.60 was generated by the model with parameters of rbf, C=1, balanced, and scale. Moreover, accuracy scores of 0.58, 0.60, 0.59, 0.40, 0.33, 0.54, and 0.54 were obtained from the PCA-SVM combination with different parameter variations. Figures 5 show the confusion matrix of all the models. The most optimal results obtained by the combination of PCA-SVM with parameters of rbf; C=1; balanced; and scale as well as its confusion matrix are presented in Figure 5(a) The number of COVID-19, normal, TB, and Viral Pneumonia cases that were classified correctly was 18 out of 51, 110 out of 144, 12 out of 38, and 67 out of 147, respectively.

3.4. Implementation Expert Sytem Diagnosis

All coding was carried out with Python programming language in Visual Studio Code using MySQL as a database. The login page can be used by specialists to access the initial system. Figures 6 shows the login page view.

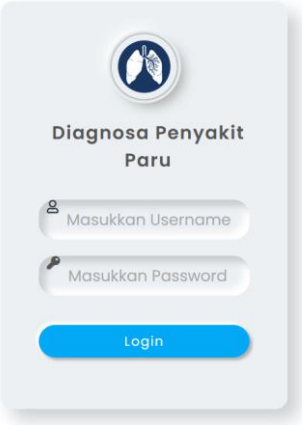

Fig. 6. Login page.

The lung specialist doctor must enter the username and password before accessing the Lung diagnostic system. When the doctor enters the wrong details, the system rejects the login request, and vice versa. Figure 7 shows the home page when the doctor is successfully logged in.

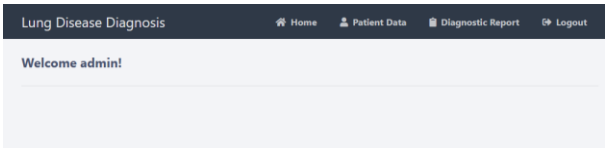

Fig. 7. Home Page

The specialists must enter patients' data first before making a diagnosis of the disease suffered by the patients. Data required include name, age, gender, contact, address, and the results of a CXR. Figure 8 shows the patients' data form that should be input.

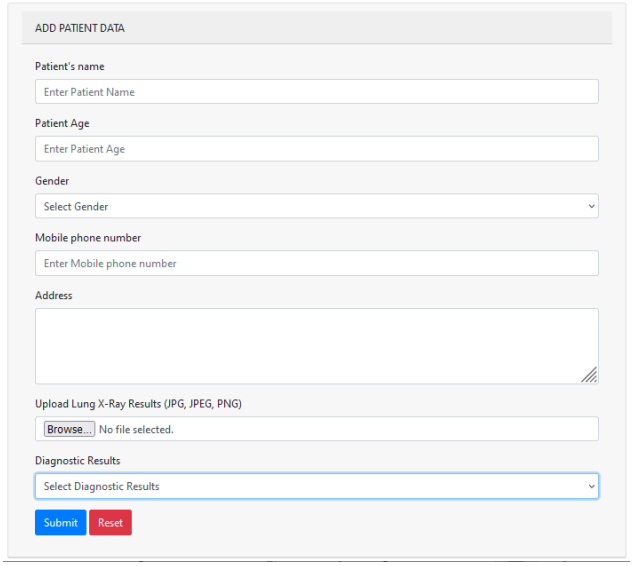

Fig. 8. Add Patients' Data Page

When the specialist enters the CXR results, the patients' illness can be predicted by pressing the prediction button. Furthermore, the data entered into the database can be saved by pressing the submit button. The results of diagnosis carried out by the specialist are stored in the database, and they are presented as an output report to be given to the patients. Figure 9 shows the report for the diagnosis of lung disease.

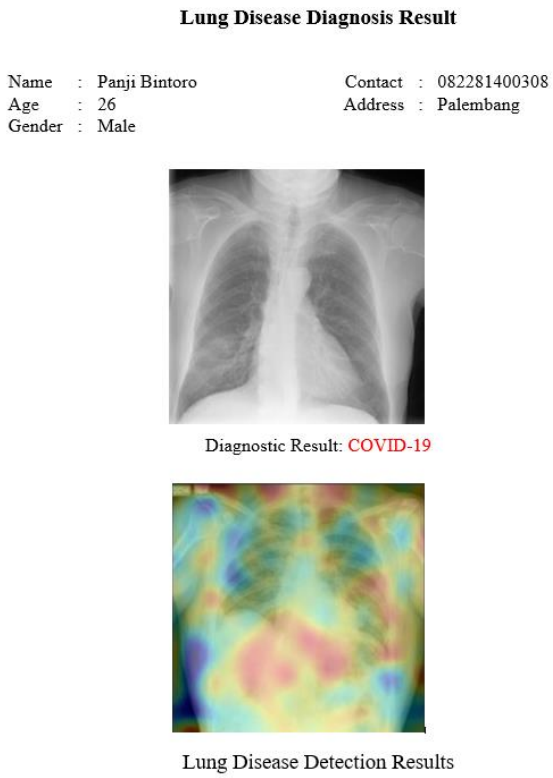

Fig. 9. Lung Disease Diagnostic Output Report

The lung disease diagnosis output report is the final result given to lung disease patients. Subsequently, specialist doctors act to provide care and healing to the patients.

4. Conclusion

This study presented a review, comparison, and discussion of the CNN and SVM architectural models. A comprehensive study was systematically carried out to investigate the effect of different transfer learning structures with traditional CNN for diagnosing lung disease. The proposed architecture models include AlexNet or Traditional, VGG16, VGG19, ResNet50, ResNet101, InceptionV3, and SVM with various parameters. The test and evaluation results showed that the CNN InceptionV3 was the best model for classifying lung disease X-ray images.

The COVID-19, Viral Pneumonia, Bacterial Pneumonia, TB, and Normal pictures had classification accuracy, precession, recall, and f1-scores that were, respectively, 0.86, 0.91, 0.91, and 0.91. This fatal lung illness causes millions of deaths every year. After a disease is diagnosed, many lives can be saved with prompt action and the right treatment plan. In addition, because radiologists and specialists have varying levels of competence, there is a lot of variety in the input images from the X-ray machine. By successfully training itself using somewhat less complicated data sets, such as pictures, with less bias and higher generalizability, InceptionV3 demonstrated good performance in categorizing COVID-19, Viral Pneumonia, TB, Normal, and Bacterial Pneumonia. This computer-assisted diagnostic tool can help radiologists and other specialists recognize these issues and take more clinically valuable images.

Acknowledgment

This research was partially supported in part by Aisyah University Indonesia, Lampung University, Binus University Indonesia, and Prima Nusantara Bukittinggi University.

References

[1] B. Y. Elhabil and S. S. Abu-Naser, “An Expert System for Ankle Problems,” Int. J. Eng. Inf. Syst., vol. 5, no. 4, pp. 57–66, 2021, [Online]. Available: https://philpapers.org/rec/YELAES

[2] A. A. Mohammed, K. Ambak, A. M. Mosa, and D. Syamsunur, “Expert system in engineering transportation: A review,” J. Eng. Sci. Technol., vol. 14, no. 1, pp. 229–252, 2019.

[3] S. Safiri et al., “Burden of chronic obstructive pulmonary disease and its attributable risk factors in 204 countries and territories, 1990-2019: Results from the Global Burden of Disease Study 2019,” BMJ, 2022, doi: 10.1136/bmj-2021-069679.

[4] F. Hussein et al., “Hybrid CLAHE-CNN Deep Neural Networks for Classifying Lung Diseases from X-ray Acquisitions,” Electronics, vol. 11, no. 19, p. 3075, 2022, doi: 10.3390/electronics11193075.

[5] A. M. Ismael and A. Şengür, “Deep learning approaches for COVID-19 detection based on chest X-ray images,” Expert Syst. Appl., vol. 164, no. March 2020, 2021, doi: 10.1016/j.eswa.2020.114054.

[6] M. Z. Alom, M. M. S. Rahman, M. S. Nasrin, T. M. Taha, and V. K. Asari, “COVID_MTNet: COVID-19 Detection with Multi-Task Deep Learning Approaches,” 2020, [Online]. Available: http://arxiv.org/abs/2004.03747

[7] M. Y. Kamil, “A deep learning framework to detect Covid-19 disease via chest X-ray and CT scan images,” Int. J. Electr. Comput. Eng., vol. 11, no. 1, pp. 844–850, 2021, doi: 10.11591/ijece.v11i1.pp844-850.

[8] B. Giri, S. Pandey, R. Shrestha, K. Pokharel, F. S. Ligler, and B. B. Neupane, “Review of analytical performance of COVID-19 detection methods,” Anal. Bioanal. Chem., vol. 413, no. 1, pp. 35–48, 2021, doi: 10.1007/s00216-020-02889-x.

[9] World Health Organization, “Laboratory testing for coronavirus disease 2019 (COVID-19) in suspected human cases,” vol. 2019, no. March, 2020.

[10] R. Yi, L. Tang, Y. Tian, J. Liu, and Z. Wu, “Identification and classification of pneumonia disease using a deep learning-based intelligent computational framework,” Neural Comput. Appl., vol. 7, 2021, doi: 10.1007/s00521-021-06102-7.

[11] I. S. Masad, A. Alqudah, A. M. Alqudah, and S. Almashaqbeh, “A hybrid deep learning approach towards building an intelligent system for pneumonia detection in chest x-ray images,” Int. J. Electr. Comput. Eng., vol. 11, no. 6, pp. 5530–5540, 2021, doi: 10.11591/ijece.v11i6.pp5530-5540.

[12] S. M. Fati, E. M. Senan, and N. ElHakim, "Deep and Hybrid Learning Technique for Early Detection of Tuberculosis Based on X-ray Images Using Feature Fusion," Appl. Sci., vol. 12, no. 14, p. 7092, 2022, doi: 10.3390/app12147092.

[13] H. Roopa and T. Asha, "Feature extraction of chest X-ray images and analysis using PCA and kPCA," Int. J. Electr. Comput. Eng., vol. 8, no. 5, pp. 3392–3398, 2018, doi: 10.11591/ijece.v8i5.pp3392-3398.

[14] E. Ayan and H. M. Ünver, "Diagnosis of pneumonia from chest X-ray images using deep learning," 2019 Sci. Meet. Electr. Biomed. Eng. Comput. Sci. EBBT 2019, pp. 2–6, 2019, doi: 10.1109/EBBT.2019.8741582.

[15] L. N. Mahdy, A. I. B. El Seddawy, and K. A. Ezzat, "Automatic COVID-19 lung images classification system based on convolution neural network," Int. J. Electr. Comput. Eng., vol. 12, no. 5, pp. 5573–5579, 2022, doi: 10.11591/ijece.v12i5.pp5573-5579.

[16] M. Hong, B. Rim, H. C. Lee, H. U. Jang, J. Oh, and S. Choi, "Multi-class classification of lung diseases using cnn models," Appl. Sci., vol. 11, no. 19, pp. 1–17, 2021, doi: 10.3390/app11199289.

[17] E. Kesim, Z. Dokur, and T. Olmez, "X-ray chest image classification by a small-sized convolutional neural network," 2019 Sci. Meet. Electr. Biomed. Eng. Comput. Sci. EBBT 2019, pp. 5–9, 2019, doi: 10.1109/EBBT.2019.8742050.

[18] M. J. Horry et al., "COVID-19 Detection through Transfer Learning Using Multimodal Imaging Data," IEEE Access, vol. 8, pp. 149808–149824, 2020, doi: 10.1109/ACCESS.2020.3016780.

[19] F. Demir, A. Sengur, and V. Bajaj, "Convolutional neural networks based efficient approach for classification of lung diseases," Heal. Inf. Sci. Syst., vol. 8, no. 1, pp. 1–8, 2020, doi: 10.1007/s13755-019-0091-3.

[20] N. Y. Lee et al., "A case of COVID-19 and pneumonia returning from Macau in Taiwan: Clinical course and anti-SARS-CoV-2 IgG dynamic," J. Microbiol. Immunol. Infect., vol. 53, no. 3, pp. 485–487, 2020, doi: 10.1016/j.jmii.2020.03.003.

[21] M. Masud, A. E. Eldin Rashed, and M. S. Hossain, "Convolutional neural network-based models for diagnosis of breast cancer," Neural Comput. Appl., vol. 34, no. 14, pp. 11383–11394, 2022, doi: 10.1007/s00521-020-05394-5.

[22] D. A. Ragab, M. Sharkas, S. Marshall, and J. Ren, "Breast cancer detection using deep convolutional neural networks and support vector machines," PeerJ, vol. 2019, no. 1, pp. 1–23, 2019, doi: 10.7717/peerj.6201.

[23] S. Kumar, A. Negi, J. N. Singh, and A. Gaurav, "Brain Tumor Segmentation and Classification Using MRI Images via Fully Convolution Neural Networks," Proc. - IEEE 2018 Int. Conf. Adv. Comput. Commun. Control Networking, ICACCCN 2018, pp. 1178–1181, 2018, doi: 10.1109/ICACCCN.2018.8748614.

[24] Y. Xie et al., "Convolutional Neural Network Techniques for Brain Tumor Classification (from 2015 to 2022): Review, Challenges, and Future Perspectives," Diagnostics, vol. 12, no. 8, 2022, doi: 10.3390/diagnostics12081850.

[25] B. Ahmad, M. Usama, C. M. Huang, K. Hwang, M. S. Hossain, and G. Muhammad, "Discriminative Feature Learning for Skin Disease Classification Using Deep Convolutional Neural Network," IEEE Access, vol. 8, pp. 39025–39033, 2020, doi: 10.1109/ACCESS.2020.2975198.

[26] T. H. H. Aldhyani, A. Verma, M. H. Al-Adhaileh, and D. Koundal, "Multi-Class Skin Lesion Classification Using a Lightweight Dynamic Kernel Deep-Learning-Based Convolutional Neural Network," Diagnostics, vol. 12, no. 9, 2022, doi: 10.3390/diagnostics12092048.

[27] H. Sharma, J. S. Jain, P. Bansal, and S. Gupta, "Feature extraction and classification of chest X-ray images using CNN to detect pneumonia," Proc. Conflu. 2020 - 10th Int. Conf. Cloud Comput. Data Sci. Eng., pp. 227–231, 2020, doi: 10.1109/Confluence47617.2020.9057809.

[28] A. Waheed, M. Goyal, D. Gupta, A. Khanna, F. Al-Turjman, and P. R. Pinheiro, "CovidGAN: Data Augmentation Using Auxiliary Classifier GAN for Improved Covid-19 Detection," IEEE Access, vol. 8, pp. 91916–91923, 2020, doi: 10.1109/ACCESS.2020.2994762.

[29] A. Irfan, A. L. Adivishnu, A. Sze-To, T. Dehkharghanian, S. Rahnamayan, and H. R. Tizhoosh, "Classifying Pneumonia among Chest X-Rays Using Transfer Learning," Proc. Annu. Int. Conf. IEEE Eng. Med. Biol. Soc. EMBS, vol. 2020-July, pp. 2186–2189, 2020, doi: 10.1109/EMBC44109.2020.9175594.

[30] Annisa Fitria Nurjannah, Andi Shafira Dyah Kurniasari, Zamah Sari, and Yufis Azhar, "Pneumonia Image Classification Using CNN with Max Pooling and Average Pooling," J. RESTI (Rekayasa Sist. dan Teknol. Informasi), vol. 6, no. 2, pp. 330–338, 2022, doi: 10.29207/resti.v6i2.4001.

[31] Jalu Nusantoro, Faldo Fajri Afrinanto, Wana Salam Labibah, Zamah Sari, and Yufis Azhar, "Detection of Covid-19 on X-Ray Image of Human Chest Using CNN and Transfer Learning," J. RESTI (Rekayasa Sist. dan Teknol. Informasi), vol. 6, no. 3, pp. 430–441, 2022, doi: 10.29207/resti.v6i3.4118.

[32] A. Fadli, Y. Ramadhani, and M. S. Aliim, "Purwarupa Sistem Deteksi COVID-19 Berbasis Website Menggunakan Algoritma CNN," J. RESTI (Rekayasa Sist. dan Teknol. Informasi), vol. 5, no. 5, pp. 876–883, 2021.

[33] F. A. Khan et al., "Chest x-ray analysis with deep learning-based software as a triage test for pulmonary tuberculosis: a prospective study of diagnostic accuracy for culture-confirmed disease," Lancet Digit. Heal., vol. 2, no. 11, pp. e573–e581, 2020, doi: 10.1016/S2589-7500(20)30221-1.

[34] T. Rahman, M. E. H. Chowdhury, and A. Khandakar, "applied sciences Transfer Learning with Deep Convolutional Neural Network (CNN) for Pneumonia Detection Using," MDPI, J. app Sci., vol. 3233, pp. 1–17, 2020.

[35] W. Tan et al., "Classification of COVID-19 pneumonia from chest CT images based on reconstructed super-resolution images and VGG neural network," Heal. Inf. Sci. Syst., vol. 9, no. 1, pp. 1–12, 2021, doi: 10.1007/s13755-021-00140-0.

[36] B. Mandal, A. Okeukwu, and Y. Theis, "Masked Face Recognition using ResNet-50," 2021, [Online]. Available: http://arxiv.org/abs/2104.08997

[37] M. Mujahid, F. Rustam, R. Álvarez, J. Luis Vidal Mazón, I. de la T. Díez, and I. Ashraf, "Pneumonia Classification from X-ray Images with Inception-V3 and Convolutional Neural Network," Diagnostics, vol. 12, no. 5, pp. 1–16, 2022, doi: 10.3390/diagnostics12051280.

[38] A. K. Jean, M. Diarra, B. A. Bakary, G. Pierre, A. K. Jérôme, and U. B. Franche-comté, "Application based on Hybrid CNN-SVM and PCA- SVM Approaches for Classification of Cocoa Beans," vol. 13, no. 9, pp. 231–238, 2022.

[39] M. Usman, S. Ahmed, J. Ferzund, A. Mehmood, and A. Rehman, "Using PCA and Factor Analysis for Dimensionality Reduction of Bio-informatics Data," Int. J. Adv. Comput. Sci. Appl., vol. 8, no. 5, pp. 415–426, 2017, doi: 10.14569/ijacsa.2017.080551.

[40] M. Turkoglu, "COVIDetectioNet: COVID-19 diagnosis system based on X-ray images using features selected from pre-learned deep features ensemble," Appl. Intell., vol. 51, no. 3, pp. 1213–1226, 2021, doi: 10.1007/s10489-020-01888-w.

[41] M. M. Abubakar, B. Z. Adamu, and M. Z. Abubakar, "Pneumonia Classification Using Hybrid CNN Architecture," 2021 Int. Conf. Data Anal. Bus. Ind. ICDABI 2021, pp. 520–522, 2021, doi: 10.1109/ICDABI53623.2021.9655918.

[42] Ž. Vujović, "Classification Model Evaluation Metrics," Int. J. Adv. Comput. Sci. Appl., vol. 12, no. 6, pp. 599–606, 2021, doi: 10.14569/IJACSA.2021.0120670.